Monte Carlo N-Particle (MCNP) Modeling of the Cellular Dosimetry of ^{64}Cu: Comparison with MIRDcell S Values and Implications for Studies of Its Cytotoxic Effects

Zhongli Cai[1], Yongkyu Luke Kwon[1], and Raymond M. Reilly[1–4]

[1]Department of Pharmaceutical Sciences, University of Toronto, Toronto, Ontario, Canada; [2]Department of Medical Imaging, University of Toronto, Toronto, Ontario, Canada; [3]Toronto General Research Institute, Toronto, Ontario, Canada; and [4]Joint Department of Medical Imaging, University Health Network, Toronto, Ontario, Canada

^{64}Cu emits positrons as well as β^- particles and Auger and internal conversion electrons useful for radiotherapy. Our objective was to model the cellular dosimetry of ^{64}Cu under different geometries commonly used to study the cytotoxic effects of ^{64}Cu. **Methods:** Monte Carlo N-Particle (MCNP) was used to simulate the transport of all particles emitted by ^{64}Cu from the cell surface (CS), cytoplasm (Cy), or nucleus (N) of a single cell; monolayer in a well (radius = 0.32–1.74 cm); or a sphere (radius = 50–6,000 μm) of cells to calculate S values. The radius of the cell and N ranged from 5 to 12 μm and 2 to 11 μm, respectively. S values were obtained by MIRDcell for comparison. MCF7/HER2-18 cells were exposed in vitro to ^{64}Cu-labeled trastuzumab. The subcellular distribution of ^{64}Cu was measured by cell fractionation. The surviving fraction was determined in a clonogenic assay. **Results:** The relative differences of MCNP versus MIRDcell self-dose S values (S_{self}) for ^{64}Cu ranged from −0.2% to 3.6% for N to N ($S_{N\leftarrow N}$), 2.3% to 8.6% for Cy to N ($S_{N\leftarrow Cy}$), and −12.0% to 7.3% for CS to N ($S_{N\leftarrow CS}$). The relative differences of MCNP versus MIRDcell cross-dose S values were 25.8%–30.6% for a monolayer and 30%–34% for a sphere, respectively. The ratios of $S_{N\leftarrow N}$ versus $S_{N\leftarrow Cy}$ and $S_{N\leftarrow Cy}$ versus $S_{N\leftarrow CS}$ decreased with increasing ratio of the N of the cell versus radius of the cell and the size of the monolayer or sphere. The surviving fraction of MCF7/HER2-18 cells treated with ^{64}Cu-labeled trastuzumab (0.016–0.368 MBq/μg, 67 nM) for 18 h versus the absorbed dose followed a linear survival curve with $\alpha = 0.51 \pm 0.05$ Gy^{-1} and $R^2 = 0.8838$. This is significantly different from the linear quadratic survival curve of MCF7/HER2-18 cells exposed to γ-rays. **Conclusion:** MCNP- and MIRDcell-calculated S values agreed well. ^{64}Cu in the N increases the dose to the N in isolated single cells but has less effect in a cell monolayer or small cluster of cells simulating a micrometastasis, and little effect in a sphere analogous to a tumor xenograft compared with ^{64}Cu in the Cy or on the CS. The dose deposited by ^{64}Cu is less effective for cell killing than γ-rays.

Key Words: dosimetry; ^{64}Cu; MCNP; MIRDcell; theranostics

J Nucl Med 2017; 58:339–345
DOI: 10.2967/jnumed.116.175695

Because it can be routinely produced in a biomedical cyclotron and emits moderate energy positrons (E_{max} = 0.653 MeV [19%]) that provide good spatial resolution (0.7 mm), ^{64}Cu is an attractive radionuclide for positron-emission tomography. The half-life of ^{64}Cu (12.7 h) is also compatible with the pharmacokinetics of peptides (*1*) or antibody fragments (*2,3*) that recognize tumor-associated receptors overexpressed on cancer cells. Moreover, many different bifunctional chelators that strongly complex ^{64}Cu have been developed for conjugation to these targeting ligands (*4*). In addition to its positron emission, ^{64}Cu emits β^- particles, Auger and internal conversion (IC) electrons, and γ-photons. The β^- particles and Auger electrons of ^{64}Cu have been studied for radiation treatment of tumors (*5–9*). The maximum β^- energy of ^{64}Cu is 0.579 MeV (40%) (*10*). These particles have a maximum range in tissues of about 2 mm and are most suitable for treatment of small tumors (*11*). The Auger and IC electrons that are emitted during the electron capture (40%) decay of ^{64}Cu have low energy (~2 keV) and only a subcellular range of less than 1 μm (*12*). These forms of radiation are most suitable for killing single cells or small clusters of cells (e.g., micrometastases). In theory, the positron emissions of ^{64}Cu may also be used to treat tumors, because the positron-emitting agent ^{18}F-FDG has been shown to have tumor growth–inhibitory effects (*13*). The nucleus (N) of tumor cells is considered to be the critical target for radiation treatment. Because the Auger and IC electrons have a subcellular range, it is important to understand the effects of subcellular distribution of ^{64}Cu on the radiation dose deposited in the N. The dose deposited by the β^- and β^+ emissions is also important, but because of their longer range, these emissions have a major cross-dose effect that can deposit dose in the N of a cell from radioactivity that is located outside the cell (e.g., in another cell or in the extracellular environment) within the 2-mm range of these particles. Various experimental geometries are used to assess the cytotoxic effects of radionuclides on tumor cells. These include single cell or monolayer geometries used in vitro (e.g., clonogenic assays), as well as small sphere geometries used in vivo in tumor xenograft mouse models. To appreciate the effects of these different geometries on the self-dose (the absorbed dose to the N from the radioactivity in the same cell) and cross-dose (the absorbed dose to the N from the radioactivity outside the cell) from ^{64}Cu, we calculated the S values (the absorbed dose per unit time-integrated radioactivity) to the N from radioactivity located at the cell surface (CS) or in the cytoplasm (Cy) or N of a single cell, in a closely packed monolayer of cells in different-sized culture plates, or in a spheric

Received Mar. 14, 2016; revision accepted Sep. 1, 2016.
For correspondence or reprints contact: Raymond M. Reilly, Leslie Dan Faculty of Pharmacy, University of Toronto, 144 College St., Toronto, ON, Canada M5S 3M2.
E-mail: raymond.reilly@utoronto.ca
Published online Sep. 22, 2016.

cluster of cells with different dimensions. These S values were calculated by Monte Carlo N-Particle (MCNP) modeling (*14*) and were compared with the values from the MIRD publication (*15*) and calculated by MIRDcell software (*16*). Previously, we found that MCNP computer code was able to assess both the self-dose and the cross-dose to the N from the Auger electron emitter ^{111}In with accuracy comparable to that by analytic methods (*17*). Finally, the survival fraction (SF) for human epidermal growth factor receptor-2 (HER2)–overexpressing MCF7/HER2-18 cells exposed in vitro to ^{64}Cu-labeled trastuzumab was determined by clonogenic assay and plotted versus the absorbed dose calculated by the MIRD schema using MCNP-calculated S values and time-integrated activity determined by cell fractionation. The survival curve of MCF7/HER2-18 cells exposed to ^{64}Cu-labeled trastuzumab was compared with that for γ-rays.

MATERIALS AND METHODS

Cell Culture and ^{64}Cu-DOTA-Trastuzumab

The human breast cancer cell line MCF7/HER2-18, stably transfected with the *HER2* gene and overexpressing HER2 (1.2×10^6 HER2/cell), was donated by Dr. Mien-Chiu Hung (MD Anderson Cancer Center, Houston) (*18*). These cells were cultured in Dulbecco's modified Eagle medium/Ham's F12 1:1MIX + antibiotics supplemented with 10% fetal bovine serum and geneticin (0.5 mg/mL; Gibco) at 37°C and 5% CO_2. Trastuzumab (Herceptin; Hoffmann-La Roche) was derivatized with 1,4,7,10-tetraazacyclododecane-1,4,7,10-tetraacetic acid mono N-hydroxysuccinimide ester (DOTA-NHS; Macrocyclics) as previously reported (*2*). Details are provided in the supplemental materials (available at http://jnm.snmjournals.org).

Clonogenic Assays and Cell Fractionation Studies

MCF7/HER2-18 cells (7×10^5 cells/well) cultured to subconfluence overnight in 6-well plates were incubated with 1.9 mL of ^{64}Cu-DOTA-trastuzumab (0–0.368 MBq/μg, 67 nM) for 18 h, then clonogenic assays were performed as previously reported (*19*). The details are provided in the supplemental materials. The SF versus the MCNP-calculated absorbed dose to the N was plotted and fit to a linear or a linear-quadratic survival curve, then compared with the survival curve of MCF7/HER2-18 cells exposed to γ-rays, which we previously found to follow a linear-quadratic model (Eq. 1):

$$SF = e^{-(\alpha D + \beta D^2)}, \qquad \text{Eq. 1}$$

where α and β were 0.823 and 0.02633 Gy^{-2}, respectively (*19*).

For subcellular uptake experiments, subconfluent MCF7/HER2-18 cells (7×10^5 cells/well) cultured overnight in 6-well plates were incubated with ^{64}Cu-DOTA-trastuzumab (0.245 MBq/μg, 67 nM) in 1.9 mL of medium for 1, 3, 15, or 18 h. For subcellular efflux experiments, subconfluent MCF7/HER2-18 cells (1.3×10^7 cells) cultured overnight in a 175 cm^2 flask were incubated with ^{64}Cu-DOTA-trastuzumab (0.245 MBq/μg, 67 nM) in 25 mL of medium for 18 h and harvested by trypsinization, then 5×10^5 cells/well were seeded and cultured in 6-well plates with 3 mL of medium per well for 9.5, 22.5, 30, and 50 h. At the end of incubation, cell fractionation was performed as previously reported to isolate the CS, Cy, or N radioactivity, which was measured in a γ-counter (*20*). Details are provided in the supplemental materials. This method provides complete separation of trastuzumab in the Cy from the N (<1%), which we validated for MCF7/HER2-18 cells by exposing similarly to Alexa-488–labeled trastuzumab (10 μg/mL) and visualizing the isolated nuclei by confocal fluorescence microscopy (Supplemental Fig. 1). We previously showed that this cell fractionation method yields nuclei without cytoplasmic contamination (*20*).

Calculation of S Values by Monte Carlo Simulation

MCNP Monte Carlo code (version 5; Los Alamos National Laboratory) (*14*) was used to estimate S values for dose deposition to the N from ^{64}Cu for a single cell, a closely packed monolayer or cluster of cells of various dimensions. The positron and β^- particle emission spectra of ^{64}Cu were taken from Lund Nuclear Data (http://nucleardata.nuclear.lu.se) whereas the spectra of the Auger and IC electrons, x-rays, and γ-photons were based on the MIRD radionuclide data (*10*). The positron, β^- particles, Auger and IC electrons, x-rays, and γ-photons, including the two 511-keV γ-photons from positron annihilation, were included in the MCNP input file to be directly sampled during the radiation transport simulation. The schematic cell geometry and modeling of ^{64}Cu distributions used in MCNP simulation were similar to our previous publication on cellular dosimetry of ^{111}In (*17*) and are shown in Figure 1. ^{64}Cu was assumed to be distributed homogeneously at the CS, in the Cy or in the N, or in 0.2-cm-thick water in a tissue culture plate (non–cell-bound ^{64}Cu). The cell and N were assumed to be concentric spheres, which fit tightly in a closely packed hexahedral universe in the case of the monolayer and cluster of cell geometries to facilitate the comparison of the S values calculated by MCNP with MIRDcell (*16*). For the purposes of the calculation, the radius of the cell and N (R_C and R_N) ranged from 5 to 12 μm and 2 to 11 μm, respectively. For simulating the exposure of cells seeded into wells in a 6-, 12-, 24-, 48-, or 96-well

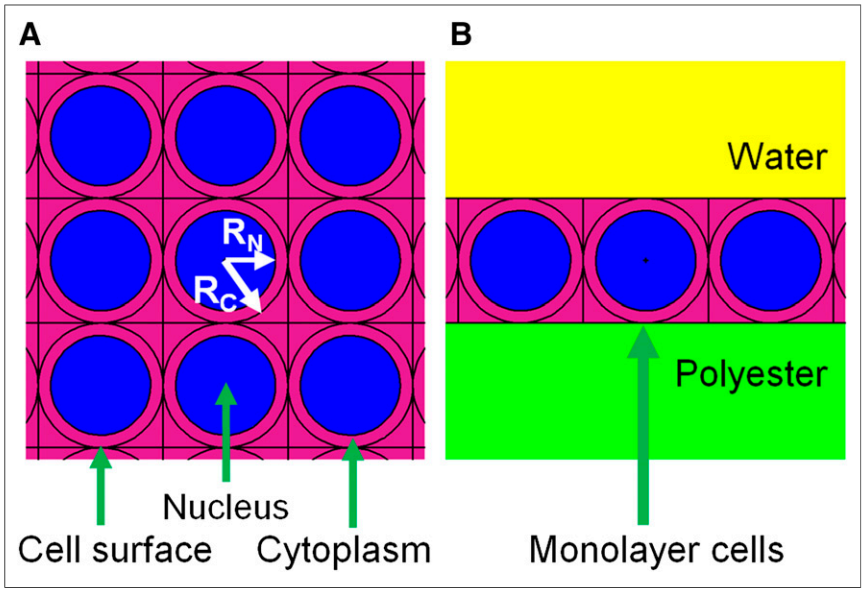

FIGURE 1. Schematic cell geometry used in MCNP simulation. (A) Top view of concentric spheres representing cell nuclei and cells, which fit tightly in a closely packed hexahedral universe in a 3-dimensional cluster or a monolayer. (B) Side view of monolayer cells in cell culture plate. R_C = cell radius; R_N = nucleus radius.

plate, the studied volume was defined as a cylinder with a radius of 1.74, 1.10, 0.77, 0.55, or 0.32 cm that contained 0.2-cm-thick water and had a 0.1-cm-thick polystyrene bottom on which a monolayer of cells, which were defined as breast tissue–equivalent phantom (ICRU-44) (*21*), was attached. To compare the MCNP results with those estimated by MIRDcell (*16*), the radius of the cylinder was set as 0.1 mm. For simulating the cluster of cells, the studied volume was defined as a sphere of breast tissue–equivalent phantom (*21*). The effect of the sphere radius (50, 100, 250, 500, 1,500, and 6,000 μm) on the S values was examined. Three types (maximum, minimum, and mean) of cross-dose S values (S_{cross}) were calculated. To simplify the calculation, with the assumption that the energy deposited to target i from source j would be equivalent to the energy deposited to target j from source i if their shape, size, and relative position were kept the same, we applied a target-source reverse approach in the calculation of the maximum and minimum S_{cross} values. For the maximum S_{cross}, the cell from which the source particles were emitted was set at the center of either the well or the sphere. For the minimum S_{cross}, the cell from which the source particles were emitted was set at the edge of either the well or the sphere farthest from the center. For the mean S_{cross}, the source particles were emitted homogeneously from either a cylinder or a sphere. The energy deposition per starting particle in all cell nuclei of the monolayer or sphere in the case of maximum or minimum S values or in the cylinder or sphere in the case of mean S values was tallied. All emitted electrons with energy less than 1 keV were assumed to deposit all their energy locally within the same cell compartment in which ^{64}Cu was located. The maximum or minimum absorbed dose to the N per starting particle was calculated by dividing the deposited energy by the mass of the N. The mean S values to either the cylinder or the sphere were calculated by dividing the deposited energy by the mass of the modeled breast tissue packed in the cylinder or sphere. The mean S values per cell were obtained by multiplying the mean S values per cylinder or sphere by cell numbers per cylinder or sphere. For each simulation, 1×10^4 to 1×10^6 particles were launched to reach an SD of less than 1% for all energy deposition results. The S_{cross} values were determined by subtracting the respective self-dose S values (S_{self}) from the total mean S values. The S_{self} values to be subtracted from the total mean S values were calculated assuming the homogeneous distribution of ^{64}Cu in a cube with the side equal to the diameter of the respective cell.

Calculation of S Values by MIRDcell

MIRDcell (version 2.0 software; http://mirdcell.njms.rutgers.edu/) (*16*) was used to calculate mean S values for dose deposition to the N from ^{64}Cu for a closely packed monolayer of cells within a 0.2-mm-diameter circle or for a 0.5-mm-diameter spheric cluster of cells. The diameter of the cell and N ranged from 10 to 24 μm and 4 to 22 μm, respectively. The predefined MIRD radionuclide ^{64}Cu and the full β-energy spectrum were chosen in the Radiation Source Table in the Source/Target tab; the N was selected as the target region; and the CS, Cy, and N were chosen as the source regions. In the Multicelluar Geometry tab, 2D Colony or 3D Cluster were selected. The distance between the cells, the percentage of cell binding, and the distribution of radioactivity among the cells were set at the cell diameter, 100%, and uniform, respectively. The maximum mean activity per cell (all cells) and time-integrated activity coefficient were set as default of 0.001 Bq and 100 h. At the completion of compute, the self-dose $S_{N\leftarrow N}$, $S_{N\leftarrow Cy}$, and $S_{N\leftarrow CS}$ were shown in the right window of the output tab, and mean activity per cell (Bq) and the corresponding mean absorbed dose to the cell (Gy) were listed on the left window of the output tab. The mean S value was obtained by dividing the mean absorbed dose to the cell by mean activity per cell and time-integrated activity coefficient 100 h × 3,600 s/h. The S_{cross} value was calculated by subtracting the S_{self} value from the corresponding mean S value.

Calculation of Mean Radiation Absorbed Dose to N

The mean radiation absorbed dose to the N was calculated on the basis of the MIRD schema (Eq. 2):

$$D = \tilde{A}_M \times S_{N\leftarrow M} + \tilde{A}_{CS} \times S_{N\leftarrow CS} + \tilde{A}_{Cy} \times S_{N\leftarrow Cy} + \tilde{A}_N \times S_{N\leftarrow N}, \quad \text{Eq. 2}$$

where, $\tilde{A}$ was the time-integrated activity in each source region (M = medium, CS, Cy, or N), and S was the MCNP-calculated mean S value for the medium or the respective cell compartments. When cells were incubated with ^{64}Cu-DOTA-trastuzumab in a 6-well plate for 18 h, the mean S values were taken from the circular monolayer model with a 1.74-cm radius packed with 7×10^5 cells (R_C = 10, R_N = 8 μm). The time-integrated activity up to 18 h in the N, Cy, and CS compartments was calculated from the area under the curve for the radioactivity versus incubation time, measured in cell fractionation studies. The time-integrated activity up to 18 h in the surrounding medium was calculated on the basis of the physical decay of ^{64}Cu using formula $A_0/\lambda \times [1\text{-exp}(-\lambda T_D)]$, where A_0 is the initial radioactivity in the medium, λ is the decay constant (1.52×10^{-5} s^{-1}) for ^{64}Cu, and T_D is the dose-integration period. Once single cells were seeded in fresh medium and cultured for 10 d to allow colony formation, the S values were taken from the single cell model. The time-integrated activity in each cell compartment up to 50 h was calculated on the basis of efflux cell fractionation experiments, after which the radioactivity was under the detection limit and thus the time-integrated activity from 50 h to 10 d was assumed to be zero.

RESULTS

Comparison of MCNP- and MIRDcell-Calculated S Values

To evaluate the differences in subcellular S values calculated by MCNP simulation versus the MIRDcell-calculated values or MIRD-published values (*15*), the S_{self} and S_{cross} values to the N for ^{64}Cu uniformly distributed in the N, Cy, or CS compartments of a single cell or cubically close-packed cells of various dimensions in a 2-dimensional circular monolayer (radius = 0.1 mm) or 3-dimensional sphere (radius = 0.25 mm) were calculated by MCNP and MIRDcell (Supplemental Tables 1–3). The relative differences of MCNP-calculated versus MIRDcell-calculated S_{self} were −0.2 to −3.7% for $S_{N\leftarrow N}$, −8.5%–3.1% for $S_{N\leftarrow Cy}$, and −11.9%–10.5% for $S_{N\leftarrow CS}$, respectively. For a single cell with a constant cell radius, as the radius of the N increased, the curve of $S_{N\leftarrow Cy}$ versus N radius exhibited a valley, but $S_{N\leftarrow CS}$ increased (Supplemental Figs. 2A and 2B), whereas for a single cell with a constant N radius, as the cell radius increased, both $S_{N\leftarrow Cy}$ and $S_{N\leftarrow CS}$ decreased (Supplemental Figs. 2C and 2D). These observations were in good agreement with the published MIRD reports and MIRDcell-calculated values (*15,16*). The relative differences of mean MCNP-calculated versus MIRDcell-calculated S_{cross} for monolayer or sphere were 26%–31% and 30%–34%, respectively. S_{cross} depended on the location of the cell within the monolayer or sphere (Figs. 2A and 2B). MCNP-calculated mean S_{cross} values were consistently larger than those calculated using MIRDcell. However, maximum and minimum S_{cross} by MCNP, as well as mean S_{cross} by MIRDcell, only slightly depended on the subcellular location of ^{64}Cu and the radius of the cell N with the maximum difference observed of 18% and 11% for MCNP and MIRDcell, respectively, both from the smallest R_C and the smallest R_N calculated (5 and 2 μm), but these differences decreased as the cell radius increased. S_{cross} decreased as the cell radius increased, following the equation of S_{cross} = constant/R_C^3 (Fig. 2).

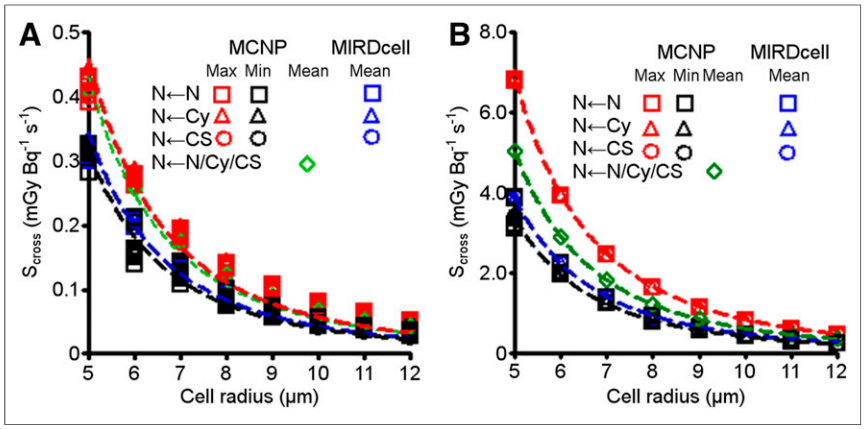

FIGURE 2. Effect of cell radius and subcellular location of ^{64}Cu on maximum, minimum, and mean S_{cross} values for cells within monolayer (0.2-mm-diameter circle) (A) and cluster (0.5-mm-diameter sphere) (B) calculated with MCNP and MIRDcell.

S Values for ^{64}Cu Under Different Experimental Conditions

The mean S values for ^{64}Cu uniformly distributed in subcellular compartments of a monolayer of cells with R_C of 5–12 μm in a single well of a 96-, 48-, 24-, 12-, or 6-well plate were calculated, then the S_{cross} values were derived by subtracting the self-dose S values from the calculated mean monolayer cell S values. The mean S_{cross} only slightly decreased (<3.2% difference between 96-well and 6-well plates) as the well size decreased (Supplemental Table 4). To examine whether the subcellular location of ^{64}Cu has an effect on the S values, the ratio of mean $S_{N\leftarrow N}$ versus $S_{N\leftarrow Cy}$ and $S_{N\leftarrow Cy}$ versus $S_{N\leftarrow CS}$ was calculated and plotted versus the ratio of R_N versus R_C for a single cell or a monolayer of cells in a 6-well plate (Figs. 3A and 3B). Both ratios decreased as the ratio of R_C/R_N increased. The ratio of mean $S_{N\leftarrow N}$ versus $S_{N\leftarrow Cy}$ was much greater than that of $S_{N\leftarrow Cy}$ versus $S_{N\leftarrow CS}$, and the difference became larger as R_C/R_N decreased. S values and S_{cross} for ^{64}Cu uniformly distributed in subcellular compartments in a spheric cell cluster (radius of 0.05, 0.1, 0.25, 0.5, 1.5, or 6.0 mm) composed of cells with R_C of 5–12 μm were calculated. The mean S_{cross} increased as the cluster size increased and R_C decreased (Supplemental Table 5), in accordance with the increased number of cells within the cluster, as listed in Supplemental Table 6. To again examine whether subcellular location of ^{64}Cu has an effect on the S value, the ratio of mean $S_{N\leftarrow N}$ versus $S_{N\leftarrow Cy}$ and $S_{N\leftarrow Cy}$ versus $S_{N\leftarrow CS}$ was calculated and plotted versus R_N/R_C (Figs. 3C and 3D). Only for the smaller spheres (e.g., radius = 50, 100, 250, and 500 μm) and R_N/R_C ratio less than 0.5 would ^{64}Cu located in the N deposit at least 1.5 times absorbed dose to the N than ^{64}Cu in the Cy. The S value to the N for ^{64}Cu uniformly distributed in 2-mm water (simulating non–cell-bound ^{64}Cu) was also determined (Supplemental Table 7).

Contribution of Radiation Emissions to S_{self} and S_{cross} Values

The contributions of γ-photon, β^- particle, positron, and Auger/IC electron emissions from ^{64}Cu to the S_{self} and S_{cross} values are shown in Supplemental Tables 8 and 9, respectively. For a single cell, the Auger/IC electrons contributed most to $S_{N\leftarrow N}$ (53%–84%), followed by β^- particles, positrons, and γ-photons, whereas the β^- particles were mainly responsible for $S_{N\leftarrow Cy}$ (45%–70%) and $S_{N\leftarrow CS}$ (73%–77%). The positrons also contributed to $S_{N\leftarrow Cy}$ (13%–21%) and $S_{N\leftarrow CS}$ (21%–24%). For a monolayer of cells attached to a well in a plate or a cluster of cells, the largest contributor to the S_{cross} were the β^- particles (67.3%–82.1%), followed by the positrons (28.9%–30.9%) and γ-photons (0.8%–1.1%). As the size of monolayer or cluster increased, the relative contribution of β^- particles to S_{cross} decreased, whereas the contribution of positrons and γ-photons increased. Figure 4 shows that the S_{cross} from β^+, β^-, and γ-photons increased with the radius of the 18-μm-diameter cell cluster, though the slope became smaller except that S_{cross} from the γ-photons continued to increase linearly with the cell cluster radius.

Clonogenic Survival Curve

The clonogenic survival of MCF7/HER2-18 cells exposed to 1.9 mL of ^{64}Cu-DOTA-trastuzumab (0–0.368 MBq/μg, 67 nM) for 18 h was determined. The subcellular distribution of ^{64}Cu in MCF7/HER2-18 cells incubated with ^{64}Cu-DOTA-trastuzumab (0.245 MBq/μg, 67 nM) for 1, 3, 15, and 18 h or treated similarly for 18 h, followed by culturing in fresh medium for 9.5, 22.5, 30, and 50 h, is shown in Figures 5A and 5B. Table 1 provides the time-integrated activity, Ã, in each source compartment (medium, CS, Cy, or N) for the 18-h incubation period, and the 10-d period allowed for colony formation. The radiation absorbed dose deposited in the N was calculated to be 3.8 ± 0.1 Gy (Table 1). The dose deposited in the N of MCF7/HER2-18 cells treated with the same concentration (67 nM) of ^{64}Cu-DOTA-trastuzumab but different specific radioactivities (0.016, 0.031, 0.061, 0.123, and 0.368 MBq/μg) was estimated to be 0.23, 0.46, 0.93, 1.86, and 5.57 Gy assuming the

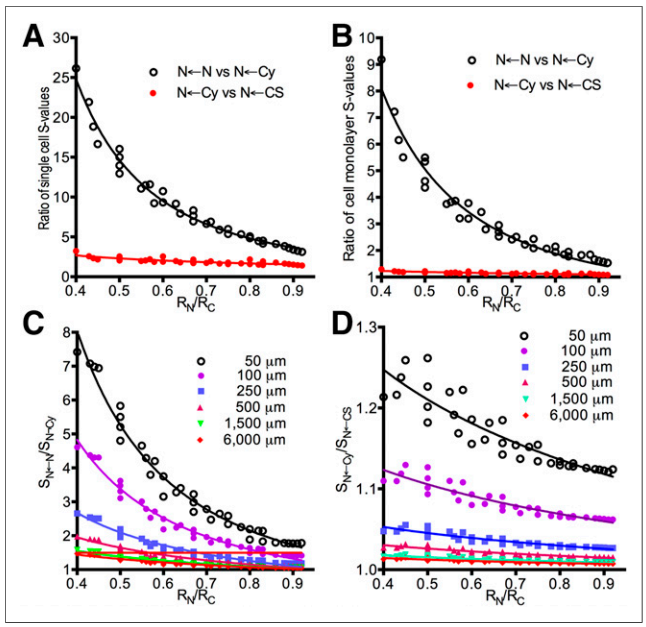

FIGURE 3. Plots of $S_{N\leftarrow N}/S_{N\leftarrow Cy}$ and $S_{N\leftarrow Cy}/S_{N\leftarrow CS}$ against R_N/R_C for single cell (A), monolayer cells in 6-well plate (B), and spheres (C and D) with radii of 50, 100, 250, 500, 1,500, and 6,000 μm, demonstrating effect of subcellular location of ^{64}Cu on S values.

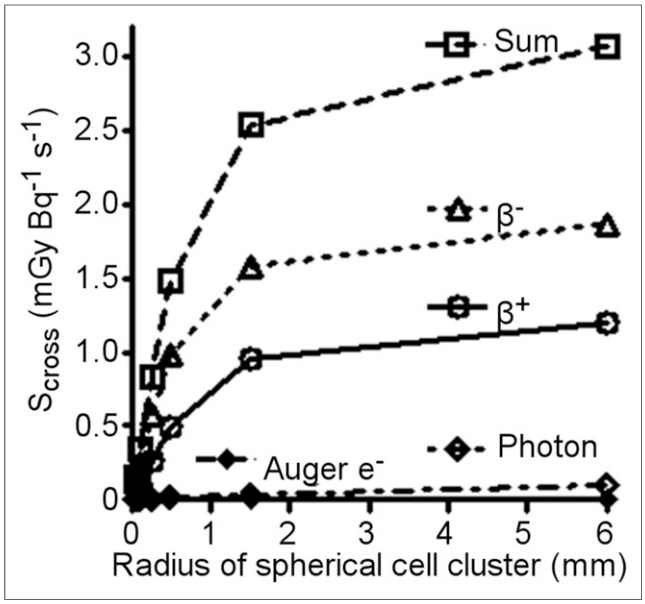

FIGURE 4. Dependence of mean S_{cross} values by sum or individual contributions of different forms of radiation emitted by ^{64}Cu on radii of spheric cluster composed of closely packed 18-μm-diameter cells.

same cellular uptake and efflux of trastuzumab. The SF versus the calculated absorbed dose to the N was plotted (Fig. 5C) and found to fit better to a linear survival curve, with an $\alpha = 0.51 \pm 0.05$ Gy^{-1} and $R^2 = 0.8838$, than a linear quadratic model. This survival curve was significantly different from the previously reported survival curve of MCF7/HER2-18 cells exposed to γ-rays, which was best fit with a linear quadratic curve with an α and β of 0.823 Gy^{-1} and 0.02633 Gy^{-2} (*19*).

DISCUSSION

In this study, we calculated S values for ^{64}Cu in a single cell, monolayer, or cell cluster geometry by MCNP simulation (*14*) and compared these values with those calculated by MIRDcell (*16*) or with the published cellular MIRD S values (*15*). Monolayer geometry is relevant to the treatment of cancer cells in vitro in a multiwell plate, whereas the cell cluster geometry applies to in vitro spheroids and in vivo treatment of tumor xenografts in mice. Although S values for single cell dosimetry (*15*) and organ macrodosimetry in humans (*22*), rats (*23*), or mice (*24*) have been published, our report is the first, to our knowledge, to describe S values for ^{64}Cu in a monolayer or cell cluster geometry. In a previous study, we found that MCNP simulation was an accurate and reliable method to assess the cellular and subcellular radiation absorbed doses from the Auger electron–emitting radionuclide ^{111}In in monolayer or cell cluster (*17*). MCNP-calculated S values for a monolayer predicted the SF of MDA-MB-468 cells exposed in vitro to ^{111}In-diethylenetriaminepentaacetic acid human epidermal growth factor based on the survival obtained by γ-radiation exposure at similar calculated doses. To assess the accuracy of MCNP for calculating the S values for ^{64}Cu, we first determined whether the MCNP-calculated S_{self} value agreed with those calculated by MIRDcell or published MIRD S values. There was good agreement between the MCNP-calculated and MIRD S values (Supplemental Table 1). We now report a comparison of the S_{cross} for ^{64}Cu calculated by MCNP or MIRDcell for cubically closely packed circular (diameter = 0.2 mm) monolayer and spheric (diameter = 0.5 mm) cluster cells (Supplemental Tables 2 and 3) by varying R_C and R_N from 5 to 12 μm and 2 to 11 μm, respectively. MCNP-calculated mean S_{cross} values were 25.8%–30.6% and 30%–34% larger than those calculated by MIRDcell for a monolayer and cluster, respectively. This was probably due to inclusion of the γ-photons in the MCNP calculation, which were ignored by MIRDcell, the difference in electron spectra, the composition of materials used, and the different calculation approach applied by MCNP and MIRDcell. Using 0.2-mm-diameter monolayer cells with R_C of 10 μm and R_N of 8 μm as an example, we calculated the S_{cross} for each of the 69 cells one by one with the same electron spectrum used by MIRDcell, defining the material of cell and cell N as water, as MIRDcell does. The average of 69 calculated S_{cross} values (Supplemental Fig. 3A) was 0.068 $mGyBq^{-1}s^{-1}$, still 25.9% larger than the value obtained by MIRDcell. In contrast, this value was only 1.4% lower than the mean S_{cross} value, suggesting that the difference was due to the different calculation approach applied. MCNP is based on Monte Carlo simulation and allows the transport

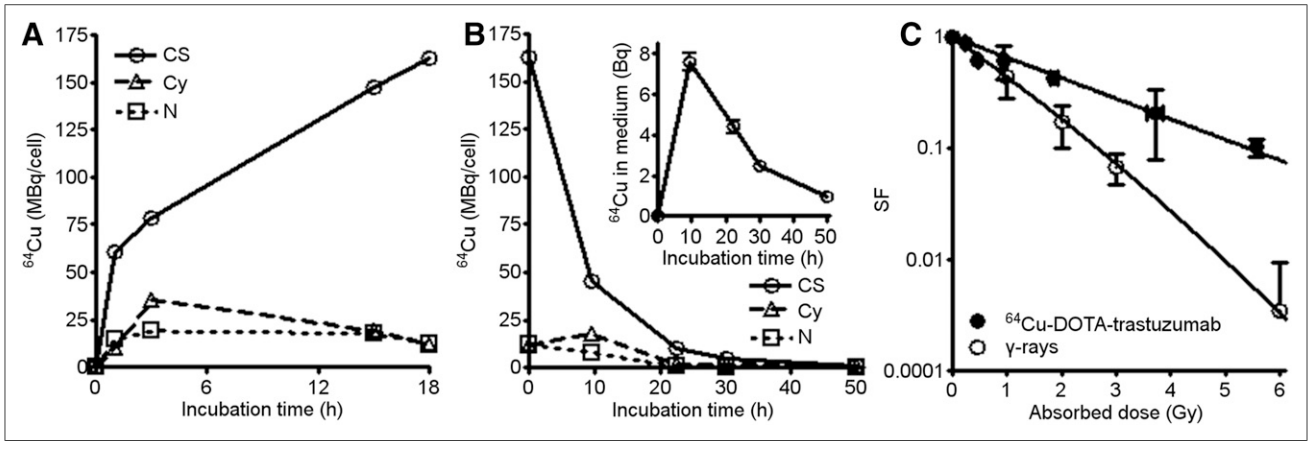

FIGURE 5. Subcellular uptake (A) and efflux (B) of ^{64}Cu by MCF7/HER2-18 cells incubated with ^{64}Cu-DOTA-trastuzumab (0.245 MBq/μg, 67 nM) as function of incubation time. Inset shows ^{64}Cu effluxed into medium. Integrated activity in each cell compartment was calculated from area under curve and was used for estimating absorbed dose to cell nucleus. (C) Survival curves of MCF7/HER2-18 cells treated with ^{64}Cu-DOTA-trastuzumab (0–0.368 MBq/μg, 67 nM) for 18 h in comparison to previously reported survival curve for MCF7/HER2-18 cells exposed to γ-rays (*19*).

TABLE 1
Estimate of Absorbed Dose to N of MCF7/HER2-18 Cells Exposed to ^{64}Cu-DOTA-Trastuzumab (0.245 MBq/μg, 67 nM) for 18 Hours, Followed by Clonogenic Assay

Source	$\tilde{A}_s$ (Bq × s)	S value ($GyBq^{-1}s^{-1}$)	D (Gy)
18-h exposure			
Cell surface	$(2.87 \pm 0.03) \times 10^4$	4.04×10^{-5}*	1.16 ± 0.01
Cytoplasm	$(6.2 \pm 0.4) \times 10^3$	5.89×10^{-5}*	0.36 ± 0.02
Nucleus	$(4.4 \pm 0.4) \times 10^3$	$2.55 \times 1\ 0^{-4}$*	1.10 ± 0.10
Medium	1.9×10^{11}	4.16×10^{-12}	0.8
10-d colony-formation			
Cell surface	$(5.3 \pm 0.3) \times 10^3$	2.96×10^{-5}†	0.157 ± 0.008
Cytoplasm	$(1.12 \pm 0.03) \times 10^3$	4.81×10^{-5}†	0.054 ± 0.001
Nucleus	$(5.9 \pm 0.1) \times 10^2$	2.44×10^{-4}†	0.145 ± 0.003
Medium	$(6.3 \pm 0.5) \times 10^5$	4.16×10^{-12}	$(2.6 \pm 0.2) \times 10^{-6}$
Total D (Gy)			3.8 ± 0.1

*Mean monolayer S values (N←CS, N←Cy, N←N), which is sum of respective self- and cross-dose S values.
†Single cell S values (N←CS, N←Cy, N←N).
$\tilde{A}_s$ = time-integrated radioactivity in source compartment.

of radiation through a 3-dimensional geometry, whereas MIRDcell uses the analytic method and propagates electrons in straight trajectories. Falzone et al. found that when the source was farther from the target region, the difference between cellular S values for Auger-emitting radionuclides calculated from PENELOPE Monte Carlo simulation and the MIRD method tended to increase (*25*).

The packing density of tumor cells in monolayer or cluster also has an effect on S_{cross}. The hexagonal closely packed spheres account for 74.0% of the cluster volume and 90.7% of the monolayer area, whereas closely packed spheres in a simple cubic lattice account for only 52.4% of the volume and 78.5% of the area. Higher packing density means more cells are included in the defined cluster or monolayer. Because this study assumed that ^{64}Cu was homogeneously distributed in each cell compartment, S_{cross} calculated using hexagonal closely packed spheres would be higher than that calculated using a cubic lattice. There are 2 reasons that we chose a cubic lattice to calculate S values: a cubic lattice is used in MIRDcell and the subconfluent monolayer cells normally occupy no more than 75% of the well area and seldom reaches 90%. Depending on the cell lines, the cell packing density both in vitro and in vivo varies but seldom reaches the highest possible density. Ideally the S_{cross} should be calculated on the basis of the known cell packing density. For dose estimation in the clonogenic assay of MCF7/HER2-18 cells, the S values were calculated on the basis of the measured cell number (7×10^5 cells per well) in a 6-well plate, which occupied only about 25% of the well area.

With positive verification of the MCNP calculation with MIRDcell, we then used MCNP to determine cellular S and S_{cross} values for monolayer cells on 96-, 48-, 24-, 12-, and 6-well plates and in a spheric cell cluster of the size (diameter of 0.1–12 mm) equivalent to a micrometastasis and typical mouse tumor xenografts (Supplemental Tables 4 and 5; Fig. 4). We also calculated the S value for ^{64}Cu uniformly distributed in 2-mm-thick water sufficient to cover cells in a well (Supplemental Table 7). These S values help to accurately calculate the absorbed doses to the cell N for cells exposed to ^{64}Cu-labeled radiopharmaceuticals during in vitro and in vivo cytotoxicity studies. Our results also inform on the design of these experiments. For example, the well size of the tissue culture plate for in vitro cytotoxicity assays is not an important factor for ^{64}Cu bound to cells, because this does not affect the absorbed doses delivered to the N. In vivo, the size of tumor xenograft needs to be considered when the therapeutic effect of ^{64}Cu agents are evaluated (Fig. 4). If the tumor is a sphere with a diameter greater than 3.0 mm, the tumor size has less effect on the absorbed dose. However, if tumor diameter is less than 3.0 mm and the time-integrated activity per tumor cell is the same, the dose decreases as tumor size decreases, due to the decreased contribution of the cross-dose.

We next examined whether the subcellular location of ^{64}Cu has an effect on the S values (Fig. 3) for a single cell, cells in a plate, or cells in a tumor xenograft. We found that the effect of subcellular location on S values was more pronounced for cells with a smaller R_N-to-R_C ratio, a single cell, followed by monolayer and small cluster cells. With the same R_N-to-R_C ratio, $S_{N\leftarrow N}/S_{N\leftarrow Cy}$ is always far larger than $S_{N\leftarrow Cy}/S_{N\leftarrow CS}$. Our results suggest that for treatment of a tumor greater than 1 mm in diameter with ^{64}Cu, it would be sufficient to simply target the tumor cells, but there would not be substantial benefit to route ^{64}Cu to the Cy or N. For treating a micrometastasis, however, it would be advantageous targeting the N to increase the dose deposited. The effect of ^{64}Cu subcellular location on the radiotoxicity observed in vitro would not be representative for a tumor larger than 1 mm in vivo.

We then examined the contribution of each radiation type to S values for a single cell, monolayer, or cluster of cells (Supplemental Tables 8 and 9). For a single cell, the subcellular location of ^{64}Cu was important for all the S values, because Auger/IC electrons contribute most to $S_{N\leftarrow N}$ (53%–84%) and substantially to $S_{N\leftarrow Cy}$ (8.2%–42%). For cells in a monolayer or in a sphere, the main contributors to the cross-dose were β^- particles, followed by positron, whereas Auger/IC electrons contributed 0.05%–5% to the S_{cross} value. Thus, only when the self-dose from Auger/IC electrons outweighed the cross-dose did the subcellular location of ^{64}Cu have an effect on the overall radiation dose deposited. Only

for monolayer and a sphere with a diameter less than 1 mm did the subcellular location of ^{64}Cu have an effect on S values (Fig. 3).

Finally, we calculated the absorbed dose to the N of MCF7/HER2-18 cells during 18-h exposure to ^{64}Cu-DOTA-trastuzumab and 10-d colony formation using the respective mean S values for monolayer cells and a single cell obtained by MCNP calculations as well as the time-integrated activity estimated from the uptake and efflux experiments. The absorbed doses to the N ranged from 0.23 to 5.57 Gy depending on the specific radioactivities of ^{64}Cu-DOTA-trastuzumab (0.016–0.368 MBq/μg). At the highest dose, the SF was 0.10 ± 0.02. Eiblmaier et al. (*26*) estimated the dose to the cell and N of A427-7 cells exposed to ^{64}Cu-TETA-Y3-TATE or ^{64}Cu-CB-TE2A-Y3-TATE using only the self-dose S value, as less than 1 Gy and 0.3 Gy, respectively, even if using high-specific-radioactivity radiopeptides (37 MBq/μg). Thus, they did not pursue further cytotoxicity experiments. However, these doses were underestimated using the self-dose S value instead of the much larger mean monolayer S values determined in our study.

We found that the survival curve of MCF7/HER2-18 cells exposed to ^{64}Cu-DOTA-trastuzumab in vitro in wells of a 6-well plate followed a linear model, which was significantly different from the previously reported survival curve of MCF7/HER2-18 cells exposed to γ-rays (Fig. 5C) (*19*), which was best fit by a linear quadratic curve. Moreover, as the dose increased, the difference between the 2 survival curves became more evident. At the same mean dose, ^{64}Cu appeared to be less cytotoxic than γ-rays. The heterogeneous distribution of ^{64}Cu-DOTA-trastuzumab bound to cells (e.g., normal or lognormal distribution) and cross-doses to cells (higher cross-dose to cells closer to the center of the well or sphere (Supplemental Fig. 3), as well as the much lower dose rates than γ-rays might account for the difference in survival curves.

CONCLUSION

S values of ^{64}Cu for closely packed monolayer and cluster cells reported here represent a valuable new contribution for dose estimation in the therapeutic application of ^{64}Cu that inform on the design of both in vitro and in vivo experiments. MCNP- and MIRDcell-calculated S values were in good agreement. Targeting ^{64}Cu into the cell N maximizes the dose to the N in isolated single tumor cells but has less effect in a cell monolayer and little effect in a sphere analogous to a tumor xenograft. ^{64}Cu appeared to be less cytotoxic than γ-rays.

DISCLOSURE

This study was supported by a grant from the Canadian Cancer Society Research Institute (grant #701682) with funds from the Canadian Cancer Society. Yongkyu Luke Kwon received a scholarship from the Canadian Institutes of Health Research Training Program in Biological Therapeutics and a MDS Nordion Scholarship. No other potential conflict of interest relevant to this article was reported.

REFERENCES

1. Lewis JS, Lewis MR, Cutler PD, et al. Radiotherapy and dosimetry of ^{64}Cu-TETA-Tyr^3-octreotate in a somatostatin receptor-positive, tumor-bearing rat model. *Clin Cancer Res.* 1999;5:3608–3616.
2. Chan C, Scollard DA, McLarty K, Smith S, Reilly RM. A comparison of ^{111}In- or ^{64}Cu-DOTA-trastuzumab Fab fragments for imaging subcutaneous HER2-positive tumor xenografts in athymic mice using microSPECT/CT or microPET/CT. *EJNMMI Res.* 2011;1:15.
3. Boyle AJ, Cao PJ, Hedley DW, Sidhu SS, Winnik MA, Reilly RM. MicroPET/CT imaging of patient-derived pancreatic cancer xenografts implanted subcutaneously or orthotopically in NOD-scid mice using ^{64}Cu-NOTA-panitumumab F(ab')$_2$ fragments. *Nucl Med Biol.* 2015;42:71–77.
4. Cai Z, Anderson CJ. Chelators for copper radionuclides in positron emission tomography radiopharmaceuticals. *J Labelled Comp Radiopharm.* 2014;57:224–230.
5. Obata A, Kasamatsu S, Lewis JS, et al. Basic characterization of ^{64}Cu-ATSM as a radiotherapy agent. *Nucl Med Biol.* 2005;32:21–28.
6. Anderson CJ, Jones LA, Bass LA, et al. Radiotherapy, toxicity and dosimetry of copper-64-TETA-octreotide in tumor-bearing rats. *J Nucl Med.* 1998;39:1944–1951.
7. Lewis MR, Wang M, Axworthy DB, et al. In vivo evaluation of pretargeted ^{64}Cu for tumor imaging and therapy. *J Nucl Med.* 2003;44:1284–1292.
8. Connett JM, Anderson CJ, Guo LW, et al. Radioimmunotherapy with a ^{64}Cu-labeled monoclonal antibody: a comparison with ^{67}Cu. *Proc Natl Acad Sci USA.* 1996;93:6814–6818.
9. Qin C, Liu H, Chen K, et al. Theranostics of malignant melanoma with $^{64}CuCl_2$. *J Nucl Med.* 2014;55:812–817.
10. Eckerman KF, Endo A. *MIRD: Radionuclide Data and Decay Schemes*. 2nd ed. Reston, VA: Society of Nuclear Medicine; 2008.
11. Reilly RM. Biomolecules as targeting vehicles for in situ radiotherapy of malignancies. In: Knaeblein J, Mueller R, editors. *Modern Biopharmaceuticals: Design, Development and Optimization*. Weinheim, Germany: Wiley-VCH; 2005:497–526.
12. Howell RW. Radiation spectra for Auger-electron emitting radionuclides: report no. 2 of AAPM Nuclear Medicine Task Group No. 6. *Med Phys.* 1992;19:1371–1383.
13. Moadel RM, Weldon RH, Katz EB, et al. Positherapy: targeted nuclear therapy of breast cancer with ^{18}F-2-deoxy-2-fluoro-D-glucose. *Cancer Res.* 2005;65:698–702.
14. Briesmeister JF. X-5 Monte Carlo Team. *MCNP: A General Monte Carlo N-Particle Transport Code*. 5th ed. Los Alamos, NM: Los Alamos National Laboratory; 2003.
15. Goddu SM, Howell RW, Bouchet LG, Bolch WE, Rao DV. *MIRD Cellular S-Values: Self-Absorbed Dose Per Unit Cumulated Activity for Selected Radionuclides and Monoenergetic Electron and Alpha Particle Emitters Incorporated into Different Cell Compartments.* Reston, VA: The Society of Nuclear Medicine; 1997.
16. Vaziri B, Wu H, Dhawan AP, Du P, Howell RW, Committee SM. MIRD pamphlet No. 25: MIRDcell V2.0 software tool for dosimetric analysis of biologic response of multicellular populations. *J Nucl Med.* 2014;55:1557–1564.
17. Cai Z, Pignol JP, Chan C, Reilly RM. Cellular dosimetry of ^{111}In using Monte Carlo N-particle computer code: comparison with analytic methods and correlation with in vitro cytotoxicity. *J Nucl Med.* 2010;51:462–470.
18. Benz CC, Scott GK, Sarup JC, et al. Estrogen-dependent, tamoxifen-resistant tumorigenic growth of MCF-7 cells transfected with HER2/neu. *Breast Cancer Res Treat.* 1992;24:85–95.
19. Cai Z, Chattopadhyay N, Liu WJ, Chan C, Pignol JP, Reilly RM. Optimized digital counting colonies of clonogenic assays using ImageJ software and customized macros: comparison with manual counting. *Int J Radiat Biol.* 2011;87:1135–1146.
20. Hu M, Chen P, Wang J, Chan C, Scollard DA, Reilly RM. Site-specific conjugation of HIV-1 tat peptides to IgG: a potential route to construct radioimmunoconjugates for targeting intracellular and nuclear epitopes in cancer. *Eur J Nucl Med Mol Imaging.* 2006;33:301–310.
21. International Commission on Radiation Units and Measurements (ICRU). *Substitutes in Radiation Dosimetry and Measurement*. Report 44. Oxford, U.K.: Oxford University Press; 1989.
22. Stabin MG, Sparks RB, Crowe E. OLINDA/EXM: the second-generation personal computer software for internal dose assessment in nuclear medicine. *J Nucl Med.* 2005;46:1023–1027.
23. Xie T, Zaidi H. Assessment of S-values in stylized and voxel-based rat models for positron-emitting radionuclides. *Mol Imaging Biol.* 2013;15:542–551.
24. Xie T, Zaidi H. Monte Carlo-based evaluation of S-values in mouse models for positron-emitting radionuclides. *Phys Med Biol.* 2013;58:169–182.
25. Falzone N, Fernandez-Varea JM, Flux G, Vallis KA. Monte Carlo evaluation of Auger electron-emitting theranostic radionuclides. *J Nucl Med.* 2015;56:1441–1446.
26. Eiblmaier M, Andrews R, Laforest R, Rogers BE, Anderson CJ. Nuclear uptake and dosimetry of ^{64}Cu-labeled chelator somatostatin conjugates in an SSTr2-transfected human tumor cell line. *J Nucl Med.* 2007;48:1390–1396.